A Direct Field Oriented Induction Machine Drive with Robust Flux Estimator for Position Sensorless Control

C. J. Bonanno *Member,* IEEE
Li Zhen *Student Member,* IEEE
Longya Xu *Senior Member,* IEEE

The Ohio State University
Departmen of Electrical Engineering
2015 Neil Avenue
Columbus, Ohio 43210

Abstract- The rotor flux is estimated for a direct field oriented induction machine drive using a voltage-current mode algorithm, or physical based algorithm. The estimated rotor flux is used to synthesize the components of the rotation matrix, $sin(\theta_e)$ and $cos(\theta_e)$. These angles are critical in transforming the command currents to the stationary frame such that field orientation is maintained. The principles of rotor flux estimation are presented, followed by examination of low speed effects, parameter sensitivity, and criteria for selection of the filter time constant, T_c. Computer simulation and extensive experimental results are included.

I. Introduction

Field oriented induction machine drives are used in industry where high precision performance is required. Currently, several research efforts are directed towards establishing *position sensorless* field oriented induction machine drives. These drives are suited for applications where drives with encoders are not practical but high performance is essential. These areas include hazardous operating environments like the process control and chemical industries.

In [1], the authors presented a rotor flux oriented, position sensorless induction machine drive. The authors proposed a solution in which simple low pass filtering of both the back emf and flux command is done, resulting in a robust flux estimator.

Fundamentally, two advantages exist in developing a position sensorless drive using the estimation approach of [1]. One, simplified control system design is employed to produce the flux estimator. Minimal time is required to tune the estimator. Two, the estimation algorithm is easily implemented in dedicated hardware or a DSP. This algorithm readily serves as a method of *medium performance motion control*, suited to variable speed applications such as pumps, blowers, compressors, etc.

However, the method of [1] employs indirect field orientation, which is sensitive to variations in the rotor time constant, T_r. The work presented in this paper differs in that the estimated rotor flux is used to synthesize the components of the rotation matrix, $sin(\theta_e)$ and $\cos(\theta_e)$, and the drive is directly field oriented. In designing a parallel filter structure based on current-voltage mode principles, the estimation of the rotor flux is insensitive to variations in the rotor time constant. The estimation algorithm in the context of a voltage-current mode operation principle is explained first, and examination of low speed effects, parameter sensitivity, and criteria for selecting T_c then follows. Computer simulation and laboratory results are included to demonstrate the soundness of the approach.

II. Rotor Flux Orientation Modeling

The symmetrical cage rotor induction machine oriented to the rotor flux is shown in Figure 1. This machine is described by a fifth order set of nonlinear differential equations:

$$\vec{V}^s_{qds} = L_\sigma \frac{d\vec{i}^s_{qds}}{dt} + R_s \vec{i}^s_{qds} + \frac{d\vec{\lambda}^s_{qdr}}{dt} \quad (1)$$

$$\vec{V}^s_{qdr} = R_r \vec{i}^s_{qdr} \mp \omega_r \vec{\lambda}^s_{dqr} + \frac{d\vec{\lambda}^s_{qdr}}{dt} \quad (2)$$

$$T_e = J \frac{d\omega_{rm}}{dt} + B_m \omega_{rm} + T_l \quad (3)$$

0-7803-3008-0/95 $4.00 © 1995 IEEE

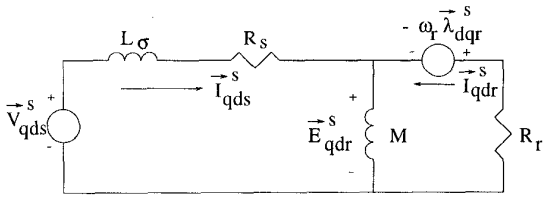

Figure 1: Rotor Flux d-q Model

where

$$M = \frac{L_m^2}{L_r} \qquad R_r = \frac{L_m^2}{L_r^2} r_r$$

$$L_\sigma = L_s - \frac{L_m^2}{L_r} \qquad R_s = r_s$$

and L_m, L_s, L_r, r_s, and r_r are the magnetizing inductance, stator and leakage inductance, and stator and rotor resistance of the induction machine oriented to the air-gap flux.

III. Estimation Principles

A. *Rotor Flux Estimator*

The block diagram of the proposed rotor flux estimator is shown in Figure 2. Faraday's law states that

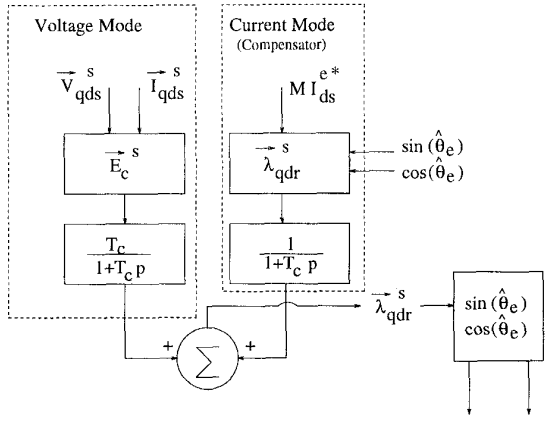

Figure 2: Flux Estimator Block Diagram

the rotor flux is the integral of the back EMF. However, the gain of an integral operator is very large at low frequencies, being infinite as frequency approaches zero (DC). This essentially makes the rotor flux estimation from pure integration of the back EMF impractical at low speeds. In addition, the back EMF is so small at low speeds that variations of stator parameters can easily corrupt the back EMF computation. The incorrectly computed back EMF, in turn, fails the rotor flux estimation. To overcome these problems, a parallel structured low pass filter is used to estimate the rotor flux as shown in Figure 2. Examining the figure, the left branch is the voltage mode component, and the right branch is the current mode component. The input to the estimator is the measured stator voltages and currents. The output is the estimated rotor flux in the stationary reference frame. Note that in a low speed range, while the back EMF is small, the magnetizing current is of normal magnitude. Therefore, the magnetizing current can be utilized to make a major contribution to rotor flux estimation. In a high speed range, the back EMF is large and more accurate. This condition naturally lends availability to rotor flux estimation, and thus the contribution of the current mode component can be reduced. The voltage mode component, which operates on the back EMF, is then dominant.

Note that Figure 2 realizes the rotor flux estimator according to the following equation:

$$\vec{\lambda}^s_{qdr} = \frac{T_c \vec{E}^s_c}{1 + T_c p} + \frac{\vec{\lambda}^{s*}_{qdr}}{1 + T_c p} \tag{4}$$

The frequency domain version of (4) is:

$$\vec{\lambda}^s_{qdr} = \frac{T_c \vec{E}^s_c}{1 + j\omega_e T_c} + \frac{\vec{\lambda}^{s*}_{qdr}}{1 + j\omega_e T_c} \tag{5}$$

where the vectors are defined as:

$$\vec{\lambda}^{s*}_{qdr} = \begin{bmatrix} \lambda^{s*}_{qr} \\ \lambda^{s*}_{dr} \end{bmatrix}, \vec{E}^s_c = \begin{bmatrix} E^s_{cqr} \\ E^s_{cdr} \end{bmatrix}, \vec{\lambda}^s_{qdr} = \begin{bmatrix} \lambda^s_{qr} \\ \lambda^s_{dr} \end{bmatrix}$$

Using the stator voltages and currents, the calculated back emf, $\vec{E}^s_c$, is given by:

$$\vec{E}^s_c = \vec{V}^s_{qds} - (R_s + j\omega_e L_\sigma)\vec{I}^s_{qds} \tag{6}$$

For notation purposes, the following expressions are introduced:

$$\vec{\mu} = \frac{1}{1 + j\omega_e T_c} = |\vec{\mu}| \angle\phi \tag{7}$$

where

$$|\vec{\mu}| = \frac{1}{\sqrt{1 + (\omega_e T_c)^2}}, \quad \angle\phi = -tan^{-1}(\omega_e T_c)$$

Then, the estimated flux expressed in (5) becomes:

$$\vec{\lambda}^s_{qdr} = \vec{\mu}\, T_c\, \vec{E}^s_c + \vec{\mu}\, \vec{\lambda}^{s*}_{qdr} \tag{8}$$

Equation (7) may be considered a vector operator, and thus equation (8) relates the rotor flux vector to a vector operator applied to the back emf and rotor flux command.

B. *Parameter Sensitivity and Low Speed Effects*

1. Parameter Sensitivity

To examine the effects of parameter sensitivity on the proposed rotor flux estimator, the nominal values of stator resistance and leakage inductance are allowed to vary. The resistance, R_s^* and inductance, L_σ^*, are related to the actual values by:

$$R_s^* = R_s - \Delta R_s, \quad L_\sigma^* = L_\sigma - \Delta L_\sigma$$

Therefore, the calculated and actual back emfs are related by

$$\vec{E}_c^s = \vec{E}_{qdr}^s + (\Delta R_s + j\omega_e \Delta L_\sigma)\vec{I}_{qds}^s \tag{9}$$

Equations (9) and (8) are combined to form:

$$\vec{\lambda}_{qdr}^s = \vec{\lambda}_1 + \vec{\lambda}_2 + \vec{\lambda}_3 \tag{10}$$

where

$$\vec{\lambda}_1 = \vec{\mu}\, T_c\, \vec{E}_{qdr}^s \tag{11}$$

$$\vec{\lambda}_2 = \vec{\mu}\, T_c\, (\Delta R_s + j\omega_e \Delta L_\sigma)\, \vec{I}_{qds}^s \tag{12}$$

$$\vec{\lambda}_3 = \vec{\mu}\, \vec{\lambda}_{qdr}^{s^*} \tag{13}$$

As can be seen, $\vec{\lambda}_2$ is the only component affected by parameter variations. In a low speed range, $\vec{\lambda}_2$ is resistive, which can be compensated for. $\vec{\lambda}_{qdr}^s$ is insensitive to L_σ since ω_e is low. As ω_e increases, $\vec{\lambda}_2$ becomes smaller and smaller as compared to λ_1. Thus, $\vec{\lambda}_1$ dominates the estimated rotor flux in a high speed range. $\vec{\lambda}_1$ is a part of the estimated rotor flux resulting from the *voltage mode* component of the parallel filter structure.

2. Low Speed Effects

The robust low speed performance of the flux estimator is explained by examining $\vec{\lambda}_1$ and $\vec{\lambda}_3$. Note that in a low speed range, $\vec{\lambda}_1$ will not be orthogonal to the back emf. The vector $\vec{\lambda}_3$, which is a part of the estimated rotor flux resulting from the *current mode* component, drives the vector $\vec{\lambda}_1$ to the correct position. Re-writing Equation (13) as:

$$\vec{\lambda}_3 = \frac{|\mu|\angle\phi}{j\omega_e}\, \vec{E}_{qdr}^{s^*} \tag{14}$$

and letting

$$\vec{E}_{qdr}^s = \vec{E}_{qdr}^{s^*} \tag{15}$$

$\vec{\lambda}_{qdr}^s$ $(\vec{\lambda}_1 + \vec{\lambda}_3)$ becomes:

$$\vec{\lambda}_{qdr}^s = |\vec{\mu}|\angle\phi\left(T_c + \frac{1}{j\omega_e}\right)\vec{E}_{qdr}^s \tag{16}$$

Note that

$$T_c + \frac{1}{j\omega_e} = \frac{1}{\omega_e|\vec{\mu}|\angle\phi}\angle -90^o \tag{17}$$

Thus

$$\vec{\lambda}_{qdr}^s = \frac{\vec{E}_{qdr}^s}{\omega_e}\angle -90^o \tag{18}$$

Equation (18) is a statement of the robust flux control existing in a field oriented drive, derived from the perspective of estimation rather than control. In a low speed range, the back EMF is small, but the synchronous speed is low as well. As the speed increases, the ratio of the back emf to the synchronous speed remains constant. Thus, the estimator is able to find the rotor flux vector which is always orthogonal to the calculated back EMF at any speed.

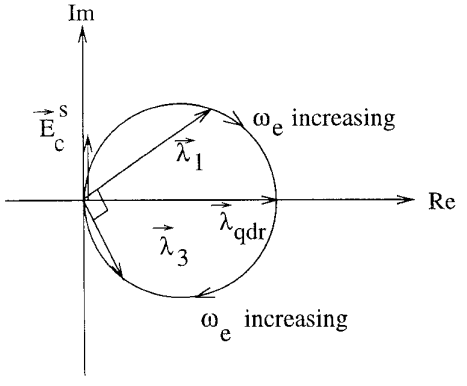

Figure 3: Phasor Diagram of Flux Estimator

A phasor diagram was constructed in Figure 3 to graphically illustrate how the components of the flux estimator are related. The locus of $\vec{\lambda}_1$ is the upper half of the circle, while the locus of $\vec{\lambda}_3$ is the lower half of the circle. As stated by equation (18), $\vec{\lambda}_1$ and $\vec{\lambda}_3$ are perpendicular at any speed. When the speed and back EMF are low, $\vec{\lambda}_1$ is tracing its trajectory and is not orthogonal to the back EMF yet. $\vec{\lambda}_3$ compensates $\vec{\lambda}_1$ and $\vec{\lambda}_{qdr}$, the estimated rotor flux, is in the correct orientation. As the speed increases, each vector nears the end of its trajectory, and the estimated rotor flux maintains its correct orientation to the back EMF.

C. *Selection of* T_c

The key design parameter for the proposed rotor flux estimator is the selection of the filter time constant, T_c, and two extremes for T_c are to be avoided.

1. Selecting T_c to be very large, or pole placement of the filter close to the origin. As the filter pole approaches the origin, the filter approximates a integrator and estimation at low speeds is difficult and very sensitive to the errors in the calculated back EMF.

2. Selecting T_c to be very small, or pole placement of the filter at synchronous speeds and beyond. This selection prevents $\vec{\lambda}_1$ from dominating at high speeds.

The possible locus of pole placement locations is shown in the complex plane in Figure 4. The optimal determination of T_c by systematic procedure is out of the scope of this paper and is skipped.

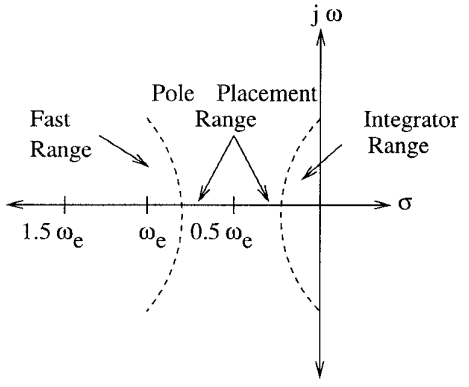

Figure 4: Selection of Tc and Pole Placement

D. *Rotor Speed Estimation*

The slip speed and synchronous speed can be calculated from the estimated rotor flux. It follows that the estimated rotor speed is the difference between the synchronous and slip speeds. The slip speed $s\,\omega_e$ in a rotor flux oriented drive is *uniquely* determined by the torque current i^e_{qs} and rotor flux magnitude $|\lambda^e_{dr}|$,

$$s\,\omega_e = \frac{R_r\, i^e_{qs}}{|\lambda^e_{dr}|} \tag{19}$$

where the torque current i^e_{qs} in the synchronous reference frame is estimated from the stationary flux components by:

$$i^e_{qs} = \frac{i^s_{qs}\lambda^s_{dr} - i^s_{ds}\lambda^s_{qr}}{\sqrt{(\lambda^s_{dr})^2 + (\lambda^s_{qr})^2}} \tag{20}$$

and the magnitude of the rotor flux obtained through:

$$|\lambda^e_{dr}| = \sqrt{(\lambda^s_{dr})^2 + (\lambda^s_{qr})^2} \tag{21}$$

The synchronous speed is also estimated from the rotor flux:

$$\omega_e = \frac{d\theta_e}{dt} \tag{22}$$

$$\theta_e = tan^{-1}\left(\frac{\lambda^s_{qr}}{\lambda^s_{dr}}\right)$$

The rotor speed, therefore, is

$$\omega_{rm} = \omega_e - s\,\omega_e \tag{23}$$

IV. Computer Simulation Results

A computer simulation was conducted of the field oriented system shown in Figure 5 to evaluate the performance of the estimator. The machine simulated has specifications listed in Table 1.

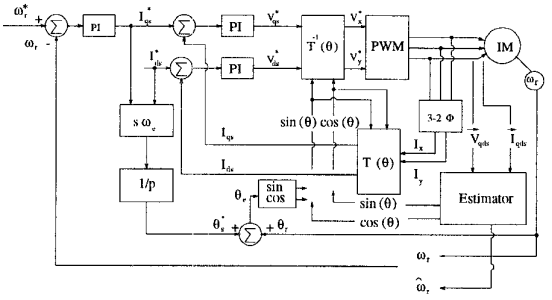

Figure 5: System Block Diagram

Table 1

220 Volts	14.8 Amps	5 HP
$L_\sigma = 3.8$ mH	M = 39.6 mH	1800 rpm
$R_s = 0.6\,\Omega$	$R_r = .3760\ \Omega$	4 poles

The low speed region is of particular interest, so a step command of 400 rpm was given to the machine. The real and estimated rotor flux are shown in Figure 6, while the real speed and phase current are shown in Figure 7.

Note the tracking of the rotor flux in Figure 6, demonstrating the effectiveness of the proposed estimation scheme.

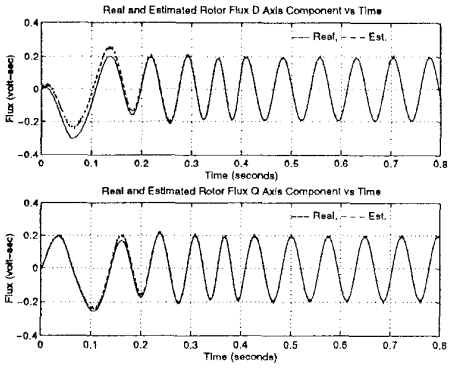

Figure 6: Real and Estimated Rotor Flux

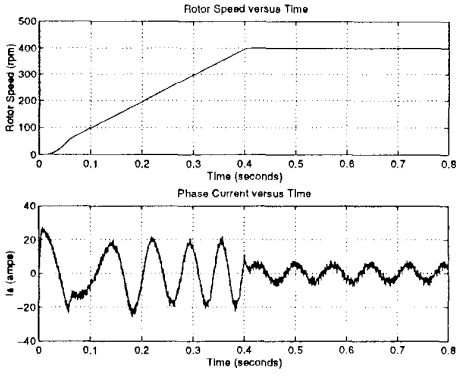

Figure 7: Rotor Speed and Phase Current

V. Experimental Results

The position sensorless induction machine system of Figure 5 has been implemented on a flexible Motorola DSP 56001 based development system [5]. The induction machine simulated by computer is used in the experiment. The DSP 56001 based controller handled the real time rotor flux estimation and torque control loop in a sampling period of 70 μsec, while the outer speed loop was sampled at 350 μsec. The very fast current and torque control is made possible due to the fact that the very concise rotor flux estimation scheme is implemented conveniently by the DSP system. The overall system is tested extensively in the OSU laboratory to verify 1) the low speed performance, 2) the robustness to variations in machine parameters, and 3) load torque disturbance rejection capability.

Figures 8 and 9 show the performance of position sensorless operation at a very low rotor speed. The top trace in Figure 8 is the rotor position in terms of electrical angle, and the bottom trace shows the

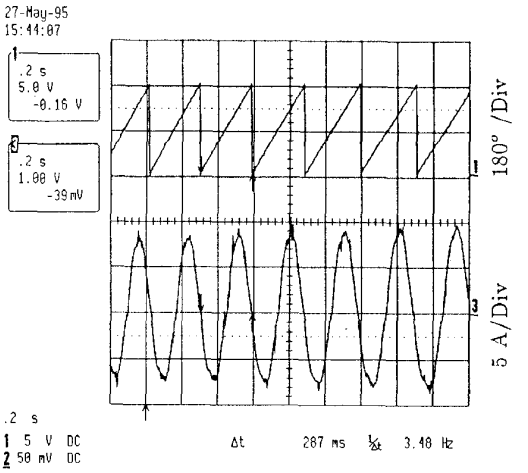

Figure 8: Electrical Rotor Angle Position and Phase Current - Low Speed (50 rpm)

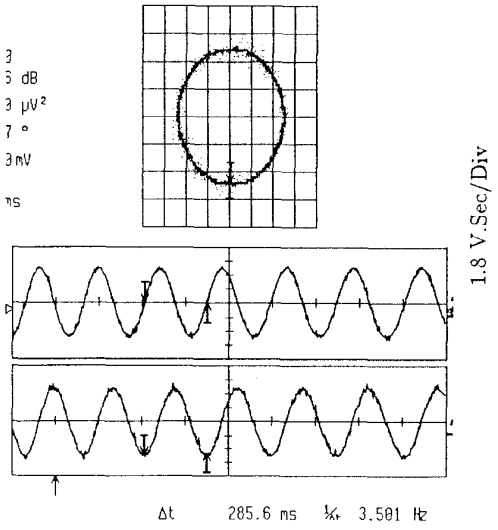

Figure 9: Estimated Rotor Flux - Low Speed (50 rpm)

stator phase current. As indicated by these traces, the induction machine is actually running at about 50 rpm, and very stable operating performance is achieved. In Figure 9, the estimated rotor flux is shown with the same operating conditions as those in Figure 8. The estimated rotor flux is displayed both along the time axis and in a polar form. This figure verifies the success of the rotor flux estimation at a very low speed.

Figure 10 shows, from the top to bottom, the real and estimated rotor speed, the estimated rotor flux, and the stator phase current during acceleration from

zero to a medium rotor speed (900 rpm). As seen, the estimated rotor speed essentially overlaps the real speed for the whole operating range, representing that a valid rotor speed estimation scheme is implemented. The constant magnitude of the estimated rotor flux combined with the variable magnitude of the phase current shows that the induction machine is truly under *position sensorless field oriented* control, since the magnitude of the rotor flux is unaffected while the stator current steps up for acceleration.

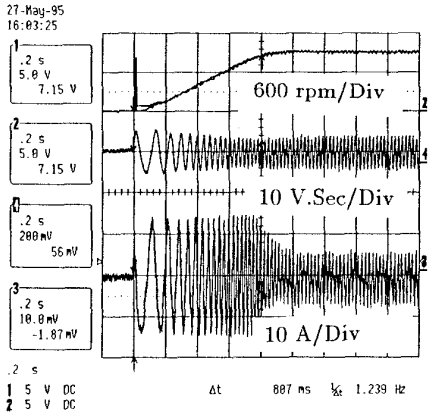

Figure 10: Real and Estimated Rotor Speed, Rotor Flux and Phase Current

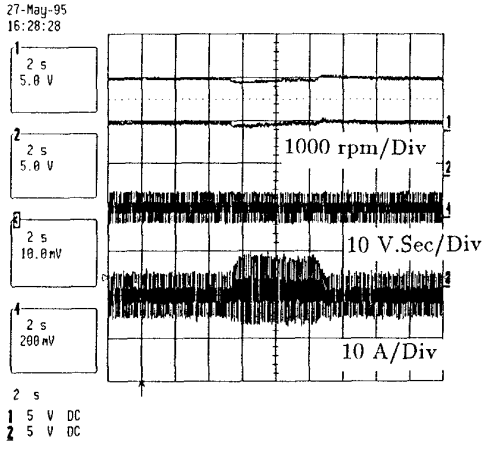

Figure 11: Real and Estimated Speed, Rotor Flux, Phase Current - Torque Disturbance

Figure 11 shows the real rotor speed, the estimated rotor speed, the estimated rotor flux, and the phase current with a load torque disturbance (0.7 rated torque). A speed dip and overshoot can be observed after a load torque is applied and removed, respectively, on both the real and estimated rotor speed traces. The speed dip and overshoot is associated with the PI gain of the rotor speed loop as identified in Figure 5. Nevertheless, the accuracy of the speed estimation is verified during the load transients. Note that during the load disturbance, the rotor flux does not change as shown by the estimated rotor flux, and decoupled control of the torque producing current from the magnetizing current is evident.

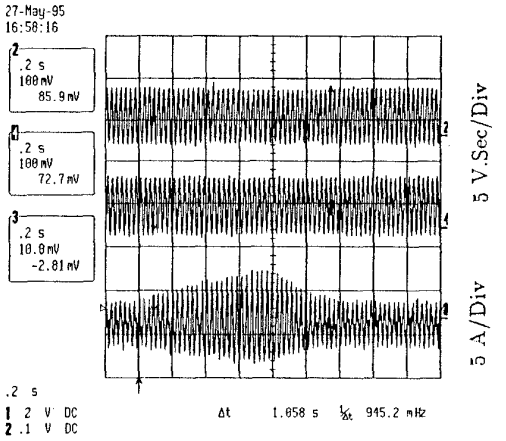

Figure 12: Rotor Flux and Phase Current - DFO System

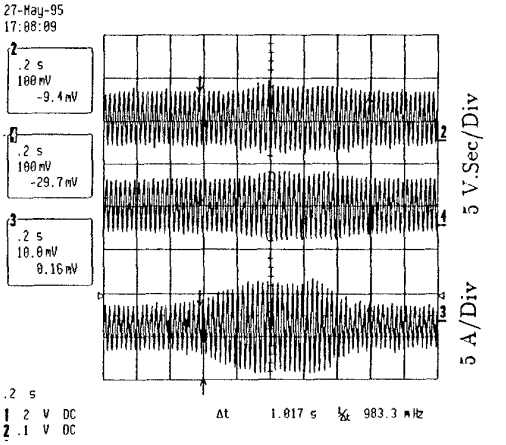

Figure 13: Rotor Flux and Phase Current - IFO System

In order to verify the robustness of the proposed position sensorless direct field oriented (DFO) control, as opposed to indirect field oriented control (IFO) with position sensor, an experiment is carried out. In both the position sensorless DFO and IFO control, the rotor time constant is doubled as compared to the well tuned conditions. Once the

machine is in steady state, a torque disturbance is applied. During the experiment, the rotor flux and stator phase current are recorded. Figure 12 shows the results in the position sensorless DFO system and Figure 13 the results for the IFO system with position sensor (from top to bottom, λ_{dr}, λ_{qr}, and i_{as} in the stationary reference frame.) As expected, the DFO system remains tuned, and the flux is not affected even with significant changes (200 percent variation) in the rotor time constant. However, in the IFO system, the rotor flux changes while the load current changes, indicating that the system is detuned. The robustness of the position sensorless DFO system and detuning of the IFO system with position sensor is more visibly seen by the flux trajectories of Figures 14 and 15. As compared to Figure 14, the magnitude of the rotor flux in the IFO system shown in Figure 15 changes substantially when the load changes. The detuning problem is evident.

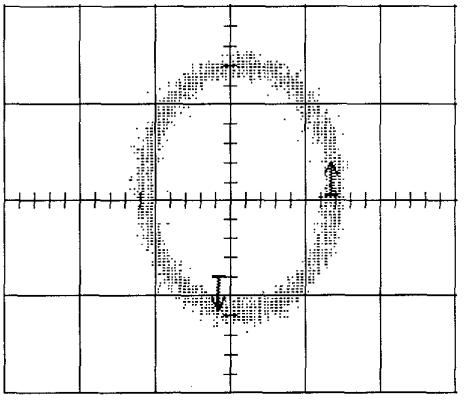

Figure 14: Flux Trajectory - DFO System

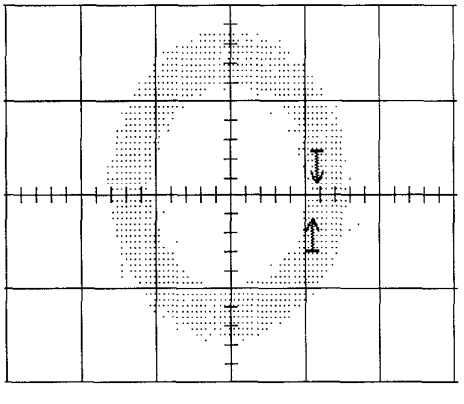

Figure 15: Flux Trajectory - IFO System

VI. Conclusions

The key issue for robust rotor flux estimation in position sensorless field oriented control is maintaining an orthogonal relationship between the estimated rotor flux and back EMF, regardless of the rotor speed and parameter variations. This is accomplished by a parallel structured rotor flux estimator. By appropriate choice of the filter time constant, T_c, sufficient compensation is given at low speed. In the high speed range, the principal component of the estimator, λ_1, becomes dominant. The choice of T_c should make the filtering algorithm active in the frequency range of operation, typically 0 to $1.5\omega_e$. Knowledge of the drive system operation dictates the parameter selection for the proposed drive, and thus the control design for the estimator is based on the physical understanding of the system. The drive is *directly field oriented*, and is robust to variations in the rotor time constant. There are no flux or speed sensors present, and the traditional problems of a direct field oriented drive are overcome. Extensive laboratory results validate the utility of the approach.

VII. Acknowledgments

The authors graciously thank Dr. Xingyi Xu of the Scientific Research Laboratory at Ford Motor Company for many insightful discussions and suggestions.

VIII. References

[1] T. Ohtani, N. Takada, and K. Tanaka, "Vector Control of Induction Motor Without Shaft Encoder," *IEEE-IAS Conference,* pages 500-507, 1989.

[2] X. Xu, and D. W. Novotny, "Implementation of Direct Stator Flux Orientation Control on a Versatile DSP Based System," *IEEE-IAS,* volume 27, number 4, pages 694-700, July/August 1991.

[3] P. L. Jansen, R. D. Lorenz, and D. W. Novotny, "Observer-Based Direct Field Orientation: Analysis and Comparison of Alternative Methods," *IEEE-IAS,* volume 30, number 4, pages 945-953, July/August 1994.

[4] C. J. Bonanno, L. Xu, and X. Xu, "Robust, Parameter Insensitive Indirect Field Orientation Control of an Induction Machine Without Shaft

Encoder," *IEEE-PESC,* Taipei, Taiwan, pages 752-757, 1994.

[5] W. Cheng, C. J. Bonanno, and L. Xu, "A General Purpose Flexible DSP 56001 Development System for Motion Control Applications," *IC-SPAT,* pages 1072-1076, 1994.

[6] R. W. De Doncker and D. W. Novotny, "The Universal Field Oriented Controller," *IEEE-IAS,* volume 30, number 1, pages 92-100, January/February 1994.

[7] H.Tajima, Y. Hori, "Speed Sensorless Field-Orientation Control of the Induction Machine," *IEEE-IAS Transactions,* Vol. 29, No. 1, pages 175-180, January/February 1993.

[8] Kubota, H., Matsuse, K., and Nakano, T., "DSP-Based Speed Adaptive Flux Observer of Induction Motor," *IEEE-IAS Transactions,* Vol. 29,No. 2, pages 344-348, March/April 1993

[9] H. Kubota, K. Matsuse, "Speed Sensorless Field-Oriented Control of Induction Motor with Rotor Resistance Adaption," *IEEE-IAS,* volume 30, number 5, pages 1219-1224, September/October 1994.

[10] F. Peng, T. Fukao, "Robust Speed Identification for Speed-Sensorless Vector Control of Induction Motor," *IEEE-IAS,* volume 30, number 5, pages 1234-1240, September/October 1994.